# Performance Analysis of a Francis Turbine under Various Operating Conditions using CFD

*Prashant Kumar*[1*], *Sunil Kumar Singal*[1], and *Pankaj Gohil*[2]

[1]Department of Hydro and Renewable Energy, Indian Institute of Technology Roorkee, 247667, India
[2]Mechanical Engineering Department, Sarvajanik College of Engineering and Technology, Surat, 395001, India

**Abstract.** Hydropower is one of the most efficient renewable energy technologies. The reaction turbines have application in very wide range of hydro power projects. The turbines are main important components of any hydro power plant. The accurate prediction of hydraulic turbine performance is a critical task for maximum amount of energy generation in plants. This study presents a comprehensive computational fluid dynamics analysis of Francis turbine operating under part load, upper part load, rated load, and overload conditions. A three-dimensional model of Francis turbine was developed using its actual geometric parameters, and simulations were conducted in ANSYS CFX with SST turbulence model. Boundary conditions are based on the operating parameters, were applied to capture the pressure and velocity distribution, and to plot hydraulic efficiency curve at different guide vane openings. The simulation results were validated against available experimental test data, showing strong agreement. The fluid flow visualization by pressure contour and velocity streamlines revealed flow separation and vortex formation patterns at off-design conditions. The findings provide valuable insights for hydropower operators to future analyses of Francis turbine performance across different operating conditions.

## 1 Introduction

Energy efficiency has become a key focus in modern power generation, particularly in the hydropower sector, which remains one of the most reliable renewable energy sources globally. Hydropower has played a significant role in the economic development of many nations. It offers lower environmental impacts than other renewable energy sources. In 2024, the global installed capacity grew by 1.5%, reaching 1418 GW [1]. Hydropower stations in India having an installed capacity of up to 25 MW are classified as small hydro plants [2]. Hydro turbines are a primary component for converting the available water power into mechanical power to generate electricity in a powerhouse. The turbines are constructed for a certain design head, flow rate, and speed. Hydraulic efficiency is a key performance parameter of hydro turbines. It is the ratio of actual hydraulic power transferred to the runner

* Corresponding author: erprashant028@gmail.com

to total water power at turbine inlet. The hydraulic turbine efficiency, $\eta_h$ [%], is represented as (Eq. (1));

$$\eta_h = \frac{T\,\omega}{(P_{inlet} - P_{outlet})Q} \quad (1)$$

where T is torque [N-m], ω is angular speed [rad /s], Q is flow rate [$m^3$ /s], P inlet is inlet pressure [kPa], and P outlet is outlet pressure [kPa]. In hydropower plants, around 60% of turbines are reaction turbines, especially Francis turbines, which are extensively used due to a wide range of head applications [3]. The turbine efficiency directly influences the hydropower plant's performance, making accurate prediction and optimization of turbine behaviour for maximizing energy output.

Numerous studies have focused on optimizing runner design and evaluating turbine performance. Kumar et al. [4] carried out the Francis turbine performance operating under different guide vane angles to identify the best operating point based on unit quantities. Unit curves were plotted for different input powers and guide vane angles, with the highest efficiency observed at the best efficiency point. Arispe et al. [5] focused on the parameterization of the draft tube elbow using the initial geometry of the GAMM Francis turbine model. The draft tube geometry was modified to achieve higher static pressure recovery and improved hydraulic efficiency compared to the original design. Kim et al. [6] conducted a numerical investigation by varying the induced angle on the output power performance of Francis turbine. The study revealed that the induced angle has a significant influence on the power output, making it important as a key parameter in hydraulic turbine design.

Computational Fluid Dynamics (CFD) has emerged as a powerful tool to investigate the complex internal flow characteristics in turbine passages, providing detailed insights into velocity distribution, pressure variation, flow separation patterns, and vortex formation that are often difficult to capture experimentally. This tool serves as a virtual laboratory for hydraulic machines, as it reliably solves the governing equations. Based on the reviewed studies, it was found that limited research has been conducted to evaluate the characteristics of turbine performance under off-design operating conditions. This work presents a numerical investigation of a Francis turbine operating under part load (50%), upper part load (80%), rated load (100%), and overload (120%) conditions. A three-dimensional model of the Francis turbine was developed, and simulations were conducted using ANSYS CFX with the Shear Stress Transport (SST) turbulence model to capture the flow separation phenomena. The boundary conditions were defined based on site-specific operating parameters to determine the hydraulic efficiency characteristics curves across the full operating range. The numerical predictions were validated against available experimental data, demonstrating a strong agreement. The flow visualization results provided deeper insight into the internal flow behaviour, flow separation, and occurrence of vortex formation under off-design conditions. The findings can assist in optimizing guide vane openings, improving hydraulic efficiency under varying load conditions, minimizing performance loss and enhancing turbine durability.

## 2 Numerical Methodology

### 2.1 3-D Modelling and Meshing

A 3-D Francis turbine model was created based on its system and operating parameters. The computational domain comprises casing, stay vanes, guide vanes, runner blades, and draft

tube. The turbine has been considered as a rated power of 200 kW, discharge of 0.85 m³/s, and head of 20 m. The modelling of each turbine component was carried out using a 3-D software module, as illustrated in Fig. 1.

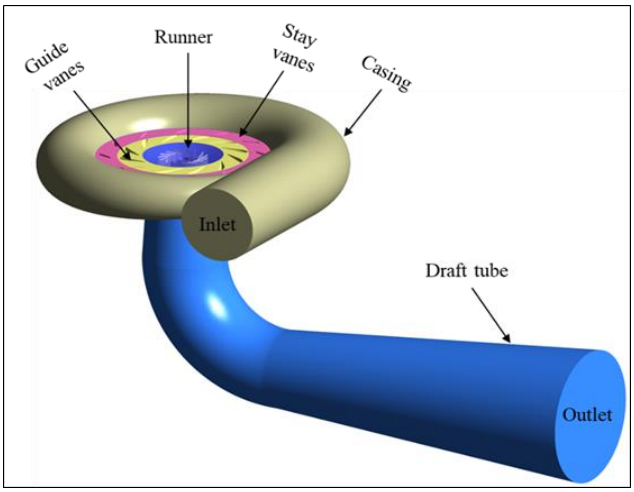


**Fig. 1.** 3-D model of Francis turbine [7].

Following the computational model, meshing software was used to generate a mesh for each fluid domain by a discretizing approach, as seen in Fig. 2.

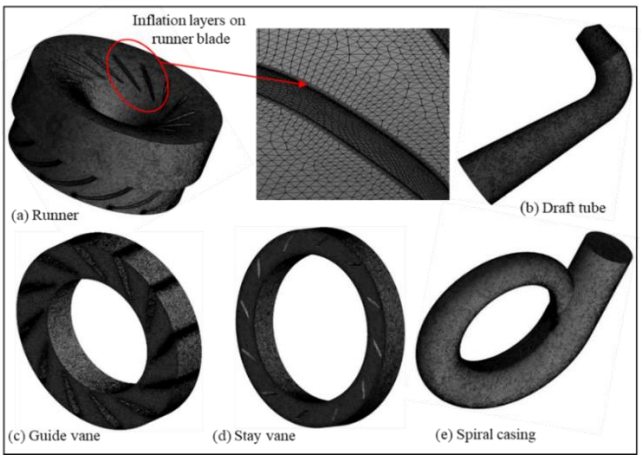


**Fig. 2.** Meshing of turbine components [8].

An unstructured tetrahedral mesh was employed due to the complex geometry of turbine. The simulation results' convergence is strongly influenced by mesh characteristics, as element quality (≤ 1), orthogonal angle (< 85), and skewness (≤ 0.9). In order to accurately capture boundary layer phenomena, the inflation layers were generated on the surfaces of runner blade.

## 2.2 Operating points and Boundary conditions

Boundary conditions must be defined to solve the governing equations. The performance characteristics of Francis turbine were evaluated by changing the guide vane angle. To get

accurate flow simulations, require appropriate boundary conditions at inlet mass flow rate and outlet static pressure are required to solve the governing equations. The details of operating and boundary conditions of Francis turbine are presented in Table 1.

**Table 1.** Considered operating and boundary conditions in the present study.

| Load condition | Guide vane angle (α) | Discharge at inlet (kg/s) | Static pressure at outlet (kPa) |
|---|---|---|---|
| Part load (50%) | 8° | 425 | 101.325 |
| Upper part load (80%) | 15° | 680 | 101.325 |
| Rated load (100%) | 20° | 850 | 101.325 |
| Overload (120%) | 32° | 1020 | 101.325 |

The runner is modelled as a rotating part operating at 750 rpm, whereas the casing, stay vanes, guide vanes, and draft tube are considered stationary. All other parts are regarded as walls with a no-slip condition. The domain interfaces are defined to connect the components, with the guide vane and draft tube linked to the runner through a frozen rotor interface. The flow separation of water is captured by employing the shear stress transfer (SST) turbulence model. The accuracy of the numerical results is affected by influential parameters, like residual criteria, iteration number, and simulation time [9]. For this study, a maximum residual convergence criterion of $10^{-5}$ were adopted to maintain numerical accuracy and stability. Furthermore, physical monitors such as hydraulic efficiency and torque confirmed a fully converged solution.

# 3 Results and Discussion

## 3.1 Mesh independence test and Performance curve

A mesh independence test was performed using five different mesh sizes: 7.42 M, 9.75 M, 12.82 M, 15.71 M, and 18.82 M, in order to optimize the computational time. The mesh refinement approach was applied to perform the independence test by using the hydraulic efficiency and $y^+$ values as shown in Fig. 3(a). As the number of mesh elements increased, the first-layer cell height decreased, which reduced the $y^+$ values across the blade surfaces. The coarse mesh showed relatively high $y^+$ values, indicating insufficient boundary layer resolution, as compared to medium and fine meshes. The test indicates that the optimum mesh size of 15.71 million elements is suitable for all simulations, as it results in a relative error of less than 1%. The efficiency obtained with this mesh size closely matches the experimental results while maintaining acceptable mesh quality. In order to achieve the performance characteristic curve or efficiency curve, simulations have been carried out under different operating conditions at a constant runner speed of 750 rpm, as shown in Fig. 3(b). The efficiency of the turbine is found to increase as the guide vane opening increases, reaching a peak at approximately 90.26%, after which it begins to decline. A comparison between the numerical results and experimental test data shows a discrepancy of about 1.09% at rated load.

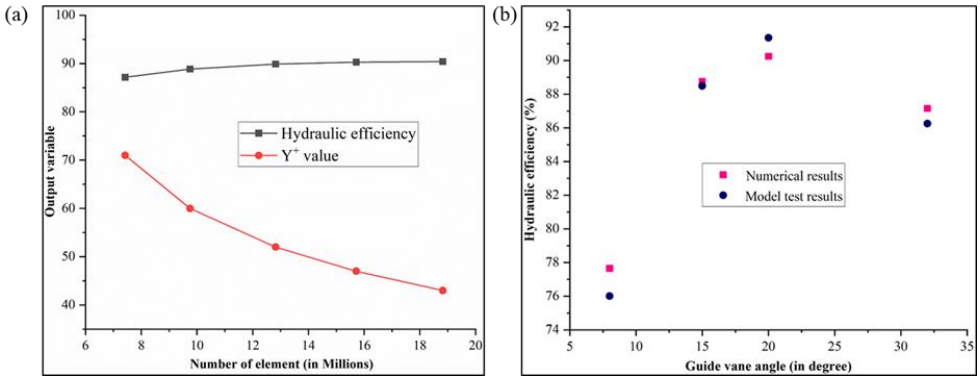


**Fig. 3.** (a) Mesh independence limit test. (b) Efficiency variation with guide vane openings.

### 3.2 Pressure energy and velocity distribution across the turbine

Pressure contours were plotted across the turbine, and it was observed that there was a decrease in pressure energy from the turbine inlet to outlet as per the turbine geometry. The water flow exiting the guide vane impinges on the pressure side of the runner blade at the leading edge. As the fluid travels along the curved surface, the pressure energy is gradually dissipated and transformed into kinetic energy. The highest pressure zone is observed on the pressure side near the leading edge, whereas the lowest pressure region develops on the suction side near the trailing edge, making this region more prone to cavitation. Fig. 4 shows the variation of pressure energy across the Francis turbine.

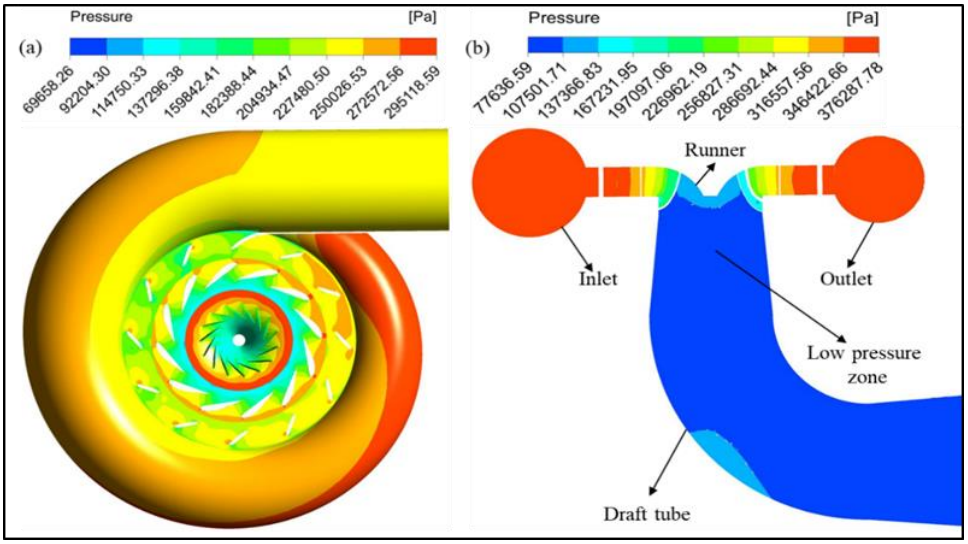


**Fig. 4.** Pressure energy distribution across the turbine.

However, the velocity contour shows that the velocity first increases at guide vane exit, then decreases as it transfers energy to the runner blades. Velocity appears higher at the trailing edge of runner blades, which may be prone to the silt erosion effect. Fig. 5 shows the variation of velocity distribution across the Francis turbine.

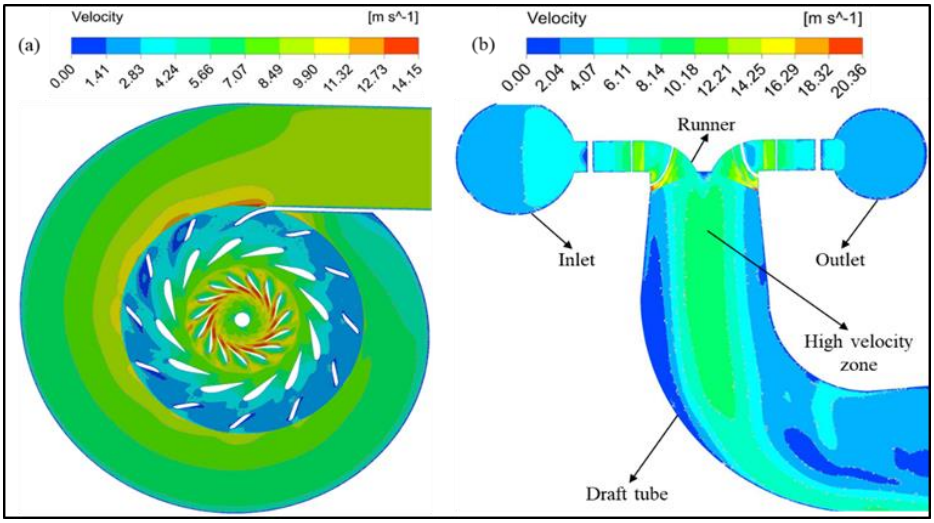


**Fig. 5.** Velocity distribution across the turbine.

### 3.3 Pressure and velocity streamline across the runner blade to blade

The pressure energy fluctuations are significant due to vortex formation and flow separation inside the runner blades at part load (GVO = 8°) and upper part load (GVO = 15°). Hence, this can lead to increased pressure pulsations in the vane less space of the hydro turbine [10]. At overload condition (GVO = 32°), excess water enters the runner, creating high turbulence. The variation of pressure energy increases due to fluid flow separation at the trailing edge, as shown in Fig. 6d. The pressure energy variation between the blades is illustrated in Fig. 6.

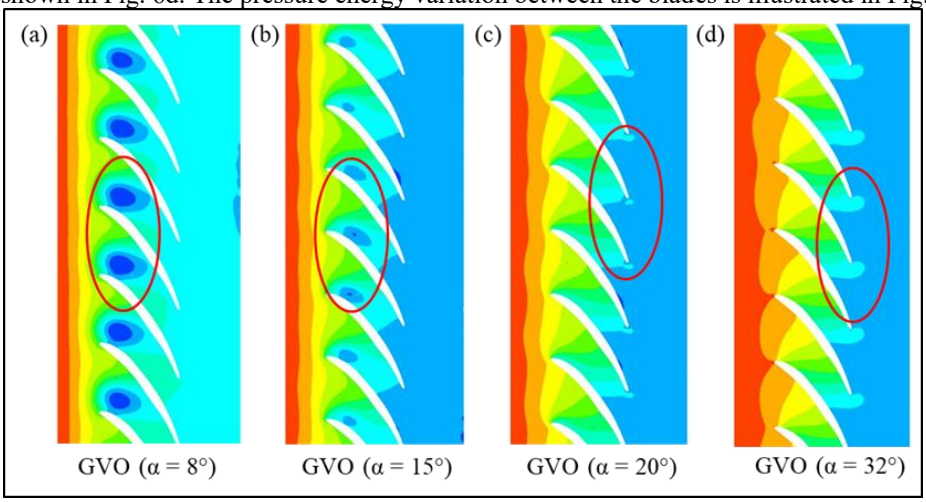


**Fig. 6.** Blade-to-blade pressure variation; (a) part load, (b) upper part load, (c) rated load, (d) overload.

The absolute velocity within the turbine can be visualized through streamlines between the blades, which indicate the direction of fluid particle velocity. Under part-load conditions, the water velocity is lower, resulting in adverse flow behaviour and increased turbulence area, as shown in Fig. 7a. The rated load (GVO = 20°) indicates the most consistent or stable flow condition, and maximum fluid flow velocity was observed at the overload condition. The variation of velocity streamlines around the blade-to-blade is shown in Fig. 7.

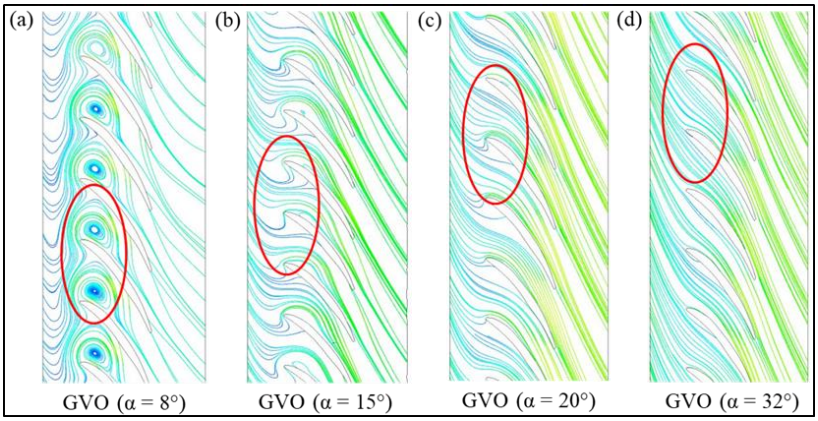


**Fig. 7.** Blade-to-blade velocity streamlines; (a) part load, (b) upper part load, (c) rated load, (d) overload.

### 3.4 Blade loading curve and Head loss in the turbine

Plotting the runner blade loading curve at different operating conditions to analyse pressure fluctuations and their effect on power output. In Fig. 8(a), the graph curve, X-axis represents the stream wise position, while Y-axis denotes the pressure coefficient of runner blade from the leading to trailing edge. It was observed that pressure variations are more noticeable on the pressure side of the runner blade than suction side. Under overload conditions, a sudden pressure drop occurs at the suction side, which could cause cavitation on the blades. Fig. 8(b) presents the graphical representation of head loss across different components of Francis turbine at various guide vane openings, computed through numerical analysis.

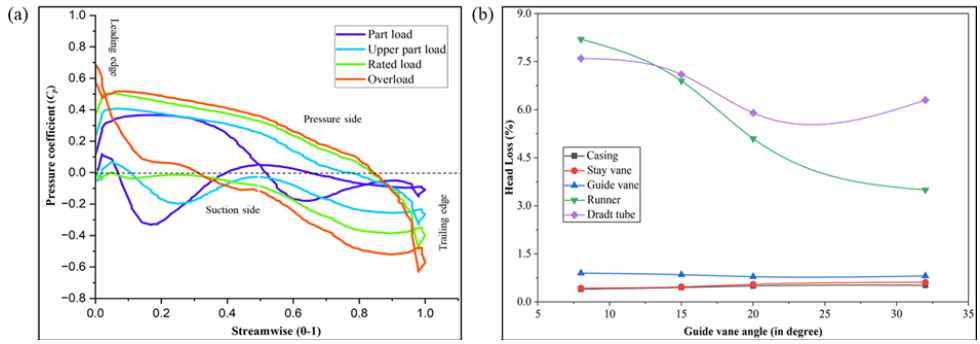


**Fig. 8.** (a) Turbine blades loading curve. (b) Head loss in Francis turbine components.

It was observed that the head loss in casing, stay vanes, and guide vanes is comparatively lower than the runner and draft tube. The casing exhibits a marginal increase in head loss with load, due to frictional effects. In contrast, the runner and draft tube experience higher head losses at part load and overload conditions, while the minimum values are recorded near the rated load.

## 4 Conclusions

In this paper, a numerical study of a Francis turbine was performed to evaluate the efficiency curve and to visualize velocity distribution, pressure variation, and flow separation patterns

under part load (50%), upper part load (80%), rated load (100%), and overload (120%) conditions. The hydraulic performance curve indicates that the hydraulic efficiency initially increases with load, reaching a maximum of 90.26% at (GVO = 20°). Beyond this point, efficiency begins to decline with further load increases. The minimum deviation in turbine efficiency is 1.09% at rated load, whereas the maximum deviation of 1.64% occurs under part-load conditions. The CFD results were validated against the manufacturer's model test data. It was also observed that the pressure energy decreases at the trailing edge of runner blade, making it more subject to cavitation under part-load conditions. Conversely, at overload conditions, the flow velocity increases along the pressure side, which is more prone to the risk of silt erosion. The most stable or uniform with less separation flow condition was recorded at rated load, whereas highly adverse flow behaviour was noted at part or/and upper part load condition. The minimum head loss was found in the computed fluid domain when the turbine is operated at the rated load condition. This study will help researchers in determining energy efficiency factors such as hydraulic characteristics, design parameters, and operating conditions of Francis turbines.

## References

1. S. Jenniches, Assessing the regional economic impacts of renewable energy sources - A literature review, Renew. Sustain. Energy Rev. **93**, 35 (2018)
2. O. Doso and S. Gao, An overview of small hydro power development in India, AIMS Energy **8**, 896 (2020)
3. P. Kumar, S. K. Singal, and P. P. Gohil, A technical review on combined effect of cavitation and silt erosion on Francis turbine, Renew. Sustain. Energy Rev. **190**, 114096 (2024)
4. M. Vijay Kumar, T. Subba Reddy, P. Sarala, P. S. Varma, O. Chandra Sekhar, A. Babqi, Y. Alharbi, B. Alamri, and C. R. Reddy, Experimental Investigation and Performance Characteristics of Francis Turbine with Different Guide Vane Openings in Hydro Distributed Generation Power Plants, Energies **15**, (2022)
5. T. M. Arispe, W. de Oliveira, and R. G. Ramirez, Francis turbine draft tube parameterization and analysis of performance characteristics using CFD techniques, Renew. Energy **127**, 114 (2018)
6. J.-H. Ha and C.-H. Kim, A Study on the Performance Analysis of Francis Hydraulic Turbine, J. Korean Soc. Mar. Eng. **33**, 1052 (2009)
7. P. Kumar, S. K. Singal, and P. P. Gohil, Numerical Analysis of Cavitation Characteristics of Francis Turbine at Different Runner Blade Numbers, IOP Conf. Ser. Earth Environ. Sci. **1411**, 012062 (2024)
8. P. Kumar, S. K. Singal, and P. P. Gohil, Computational Study of a Low-Head Francis Turbine with Varying Runner Blade Numbers, in (Springer, Singapore, 2025), pp. 481–494
9. F. R. Menter, Two-equation eddy-viscosity turbulence models for engineering applications, AIAA J. **32**, 1598 (1994)
10. B. R. Rode and A. Kumar, Unstable pressure fluctuations in the vaneless space of high-head reversible pump-turbines – A systematic review, J. Energy Storage **72**, 108397 (2023)